nature nanotechnology

REVIEW ARTICLE

https://doi.org/10.1038/s41565-018-0228-6

Emerging hydrovoltaic technology

Zhuhua Zhang[1,2], Xuemei Li[1,2], Jun Yin[1], Ying Xu[1], Wenwen Fei[1], Minmin Xue[1], Qin Wang[1], Jianxin Zhou[1] and Wanlin Guo[1]*

Water contains tremendous energy in a variety of forms, but very little of this energy has yet been harnessed. Nanostructured materials can generate electricity on interaction with water, a phenomenon that we term the hydrovoltaic effect, which potentially extends the technical capability of water energy harvesting and enables the creation of self-powered devices. In this Review, starting by describing fundamental properties of water and of water–solid interfaces, we discuss key aspects pertaining to water–carbon interactions and basic mechanisms of harvesting water energy with nanostructured materials. Experimental advances in generating electricity from water flows, waves, natural evaporation and moisture are then reviewed to show the correlations in their basic mechanisms and the potential for their integration towards harvesting energy from the water cycle. We further discuss potential device applications of hydrovoltaic technologies, analyse main challenges in improving the energy conversion efficiency and scaling up the output power, and suggest prospects for developments of the emerging technology.

Water is not only vital to life but also represents the largest carrier of energy on the Earth. Covering 71% of the Earth's surface, water consumes about 35% of the solar energy received by the Earth, corresponding to a remarkable 60 petawatts (10^{15} W)[1]. If just a small portion of the tremendous energy contained in water could be harvested, it would readily satisfy the global energy demand of 18 terawatts (10^{12} W)[2]. Yet, unlike other energy sources (for example wind or solar energy), water energy evolves into a rich variety of forms that dominate the energy transfer occurring in various natural phenomena. Traditional technologies can harness very little of this water energy, despite a long history of attempting to do so. As early as 400 BC, the kinetic energy of falling or running water was converted into useful mechanical energy by a water wheel, which operates by direct transfer of water momentum within the framework of classical mechanics. In the late nineteenth century, water power was used to drive electromagnetic generators for electric output, a harvesting approach founded on classical electrodynamics and now widely applied in the hydropower industry. In 1859, Quincke generated electricity from water by direct interaction between water and solid, in a process by which a flow of electrolytes under a pressure gradient through a narrow channel generates an electric voltage in the flow. Called streaming potential, this process was based on electrokinetic theory[3]. The electrokinetic conversion efficiency can be enhanced by using nanochannels with atomically smooth walls and has thus inspired interest in using nanomaterials for water energy harvesting[4–7].

Compared with bulk materials, nanomaterials are exceptionally sensitive to external stimuli and can harvest richer forms of water energy that are inaccessible by conventional technologies. Among various nanomaterials, carbon nanomaterials—represented by graphene and carbon nanotubes (CNTs)—stand out in their mature techniques for mass production of high-quality samples with different dimensionalities[8–13]. Moreover, carbon nanomaterials can expose all of their atoms on the surfaces, permitting substantial interaction with water through electronic coupling. As such, recent experiments have demonstrated electricity generation in carbon nanomaterials on exposure to water flows[14–16], waves[17] and rains[18], with no need of a pressure gradient as is required by the streaming potential. These new advances extend not only the classical electrokinetic theory[19] but also, more broadly, the capability of water energy harvesting based on traditional principles.

But more energy from water exists in an insensible form: evaporation, which draws thermal energy from the ambient environment by converting the sensible heat into latent heat[20]. The evaporation of a single gram of water converts 2.26 kJ of energy from liquid to vapour, an amount of energy close to that contained in an AAA battery. Globally, evaporation energy contains up to 66% (40 petawatts) of the total energy consumed by water, creating an average energy flux as high as 80 W m^{-2} (refs [1,21]). Though the mechanical work of converting vapour from boiling water has long been used to drive steam engines, the abundant energy that might be derived from natural evaporation has yet to be exploited. This situation has changed recently with an experiment that directly converted evaporation energy into volt-level electric voltages by using nanostructured carbon materials called carbon blacks[22]. The carbon materials enable a unique interaction with water vapour, suggesting great potential in harnessing energy from this ubiquitous source.

Generating electricity from the direct interaction of carbon nanostructures with flowing, waving, dropping and evaporating water leads to the emergence of a new energy conversion effect in the materials, which we term the hydrovoltaic effect. This effect parallels other energy conversion effects, such as the photovoltaic effect[23], but is more 'colourful' in converting diverse water energy into electric power through an electric coupling between materials and water, as testified by the large number of recent experiments. Yet, unlike other well-studied energy conversion effects, research on the hydrovoltaic effect is in its infancy and calls for continued efforts to materialize its great potential. Here, we review recent progress with this effect, mostly in carbon nanomaterials, with particular focus on evaporation-induced electricity.

Basic properties of water and water–solid interfaces

Because water is key to the hydrovoltaic effect, we first discuss its basic properties. A water molecule is formed by two hydrogen atoms covalently bonded to an oxygen atom, with an included angle of 104.5° at the oxygen. The water molecule is polarized owing

[1]Key Laboratory for Intelligent Nano Materials and Devices of Ministry of Education, State Key Laboratory of Mechanics and Control of Mechanical Structures and Institute of Nanoscience, Nanjing University of Aeronautics and Astronautics, Nanjing, China. [2]These authors contributed equally: Zhuhua Zhang, Xuemei Li. *e-mail: wlguo@nuaa.edu.cn

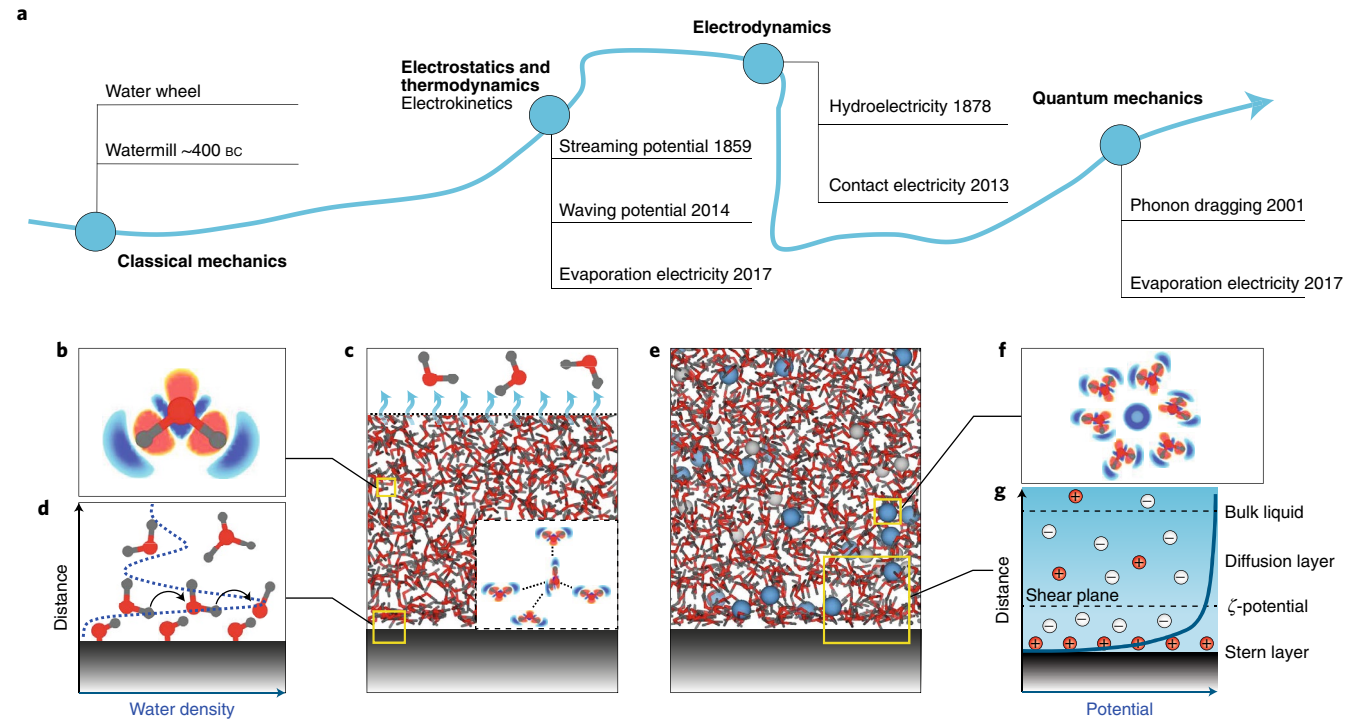

Fig. 1 | Fundamental theories of water energy harvesting and water–solid interactions. a, An evolutionary overview of the fundamental theories, from classical mechanics, thermodynamics and electrostatics, and electrodynamics, to quantum mechanics. Electrokinetics is a more specific theory for the corresponding electric phenomena, founded on thermodynamics and electrostatics. The timeline follows the shape of the Yellow River. Important advances of harvesting principles pertaining to each theory are listed. **b**, A water molecule is polarized owing to electron transfer from hydrogen to oxygen (from blue to red). **c**, Illustration of bulk water on a solid surface. In bulk water, each water molecule attracts four neighbours arranged in a tetrahedral coordination via hydrogen bonding (inset). The molecule is evaporated near the water surface when its hydrogen bonds are broken. **d**, Illustration of proton transport (indicated by curved tail arrows) near a solid surface terminated with hydroxyl groups. The dotted blue line is a typical water density profile near a solid surface. **e**, Ions dominate the interaction between aqueous solution and solid. The cations and anions are illustrated by blue and grey balls, respectively. **f**, Each ion is hydrated by attracting six water molecules. **g**, An electric double layer forms at the solution–solid interface, consisting of Stern layer and diffusion layer. The boundary between the diffusion and Stern layers is the shear plane, at which the potential is called the zeta potential. The blue line gives the electric potential profile near the interface.

to electron transfer from the hydrogen atoms to the oxygen atom (Fig. 1b), and has an electric dipole moment of 0.039*e* nm, where *e* is the electronic charge[24]. The negatively charged oxygen and positively charged hydrogen atoms in different molecules can form a hydrogen bond, H…O, when the distance between two oxygen atoms is less than 0.35 nm and the O–H…O angle is less than 30° (ref. [25]). The hydrogen bond energy is 0.16 eV (ref. [26]), which is weaker than a covalent O–H bond of 4.76 eV but stronger than a van der Waals strength of ~0.08 eV (ref. [27]). In bulk water, a hydrogen bond network around a molecule usually has a local tetrahedral coordination (inset in Fig. 1c), with two molecules acting as an acceptor and the other two acting as a donor. Each molecule links to its neighbours by at least one hydrogen bond. The dynamic process of liquid water is the making and breaking of hydrogen bonds. In an ionic solution, each monovalent ion can be hydrated by six water molecules through Coulomb attraction (Fig. 1f).

Hydrogen bonds are essential for phase transitions of water. When a water molecule near the liquid surface has enough kinetic energy to break the hydrogen bonds, it is evaporated into the air. The temperature of the liquid decreases owing to the lower kinetic energy of the remaining molecules. The liquid then absorbs heat from the environment (if open) to increase the kinetic energy of the remaining water molecules and sustain the evaporation. The strong dynamic nature of hydrogen bonds enables protons to transport within the hydrogen-bonded media[28], either from H_3O^+ to an adjacent water molecule or from a water molecule to an adjacent OH^- (Fig. 1d, solid arrows), similar to the transport of a hole carrier in semiconductors. The light mass of hydrogen endows its nucleus with strong quantum effects under moderate and low temperatures. The influence of such quantum effects on the properties of water has been extensively studied[29–33]. The quantum effects make strong hydrogen bonds stronger and weak hydrogen bonds weaker[34,35], accordingly modifying the structure of liquid water.

To understand how to effectively transfer the energy from water to solids requires an understanding of the interaction between water and solid surfaces. When water makes contact with solids, layers of water form near the interface (Fig. 1d, blue dashed line), creating detailed structures that are dependent on the wetting properties of the solid surfaces[36,37]. Water molecules form hydrogen bonds with hydrophilic substrates and thus display homogeneous structures (as schematically illustrated in Fig. 1d), whereas water interacts more weakly with hydrophobic substrates. When an aqueous solution makes contact with a solid (Fig. 1e) with surface charge, the interfacial interaction is dominated by an electric double layer (EDL)[38–40], as proposed by Helmholtz in 1853. This EDL is composed of a surface ion layer firmly adsorbed on the solid, known as the Stern layer, as well as a layer rich in counterions attracted to the surface charge, known as the diffusion layer (Fig. 1g). The EDL creates a strong electric field, resulting in a sharp potential gradient across it. The boundary between the Stern and diffusion layers is the shear plane, the electric potential of which is called the zeta potential[41]. This potential decreases in

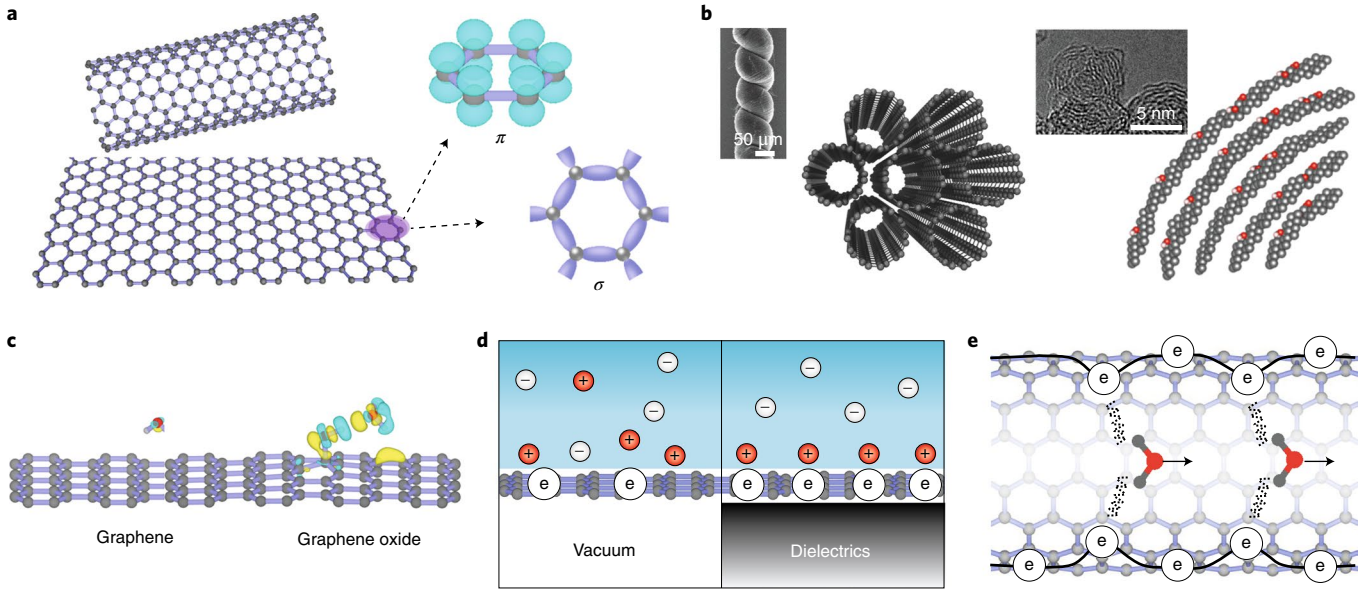

Fig. 2 | Carbon nanomaterials and carbon–water interactions. a, Atomic models of graphene and CNT, where the in-plane σ-bonds and out-of-plane π-bonds are illustrated. **b**, Microscopic images of a twisted CNT yarn (left) and carbon black (right), made up of CNT bundles and graphene flakes with oxygen (red balls) groups, respectively. **c**, Computed charge density shows little charge exchange between water and a perfect graphene lattice, but shows marked electric donation from graphene (from cyan to yellow) to water when graphene is functionalized by a hydroxyl group. **d**, Illustration of the interfaces between ionic solution and a freestanding graphene sheet, and between the solution and a graphene sheet overlaid on a dielectric substrate. **e**, Schematic illustration of electron drag induced by moving water molecules inside a CNT. Panel **b**, microscopic images, CNT yarn adapted from ref. [122], AAAS; carbon black adapted from ref. [22], Springer Nature Ltd.

magnitude with increasing ionic concentration and pH value, typically varying from −80 meV to 80 meV for NaCl solutions[42]. The distance between the shear plane and the nearest bulk liquid region is the Debye length (in the range of 1–100 nm; ref. [43]), in which the density of counter-ions decreases when moving farther from the shear plane.

Nanostructured carbon materials

Nanostructured materials have shown exceptional sensitivity to adsorbed species, as determined by the spatio-temporal energy correlation at the nanoscale. As such, they represent another key element of the hydrovoltaic effect. When the spatial scale shrinks from macroscale to nanoscale, the temporal scale will reduce to nanoseconds and even to femtoseconds. The related energy scale of an externally applied field will drop by 18 orders from joule (1 N × 1 m) to attojoule (10^{-18} J = 1 nN × 1 nm = 6.42 eV). This falls into the energy scale of the local fields of matter, consisting of orbitals, charges and spin states. Therefore, at the nanoscale, local and externally applied fields can be strongly coupled to endow materials with distinctly different behaviours from their bulk counterparts[44]. Such nanoscale multi-field couplings turn the carbon nanomaterials into functional nanostructures that are desirable for the conversion of various forms of water energy.

The most prominent carbon nanomaterial is graphene, a single layer of graphite with a honeycomb lattice. The C–C bonds are dominated by strong in-plane σ-bonds, complemented by out-of-plane π-bonds[45] (Fig. 2a). The abundant electronic properties of graphene, such as novel Dirac fermions[46], mainly stem from the π-bonds that symmetrically reside on two sublattices. All the π-bonds are exposed on the surface where they can substantially interact with external species and physical fields, making graphene a suitable material for the hydrovoltaic effect. As the π-bonds are fairly active, graphene can be functionalized by grafting various chemical groups, which then mediate its interaction with external species.

Graphene is the geometrical precursor to diverse carbon nanostructures. It can be rolled up into CNTs and fullerenes and tailored into nanoflakes. In particular, the curvature of CNTs makes most of the π-states distribute on the outer tube surface, which is thus chemically more reactive than graphene in achieving enhanced coupling with water. CNTs also provide ideal one-dimensional (1D) nanospaces for forming new water structures[47,48] and for rapid water transport[49–51]. Early simulations suggest that the proton mobility along water chains in CNTs is 40 times higher than in bulk water[52]. CNTs and graphene can be further assembled into 3D nanostructured carbon materials, including CNT films, fibres[53,54], sponges, foams and carbon blacks[55] (Fig. 2b). The constituent carbon elements in these materials interact with one another mainly through van der Waals interaction and thereby inherit key properties from graphene. In particular, carbon black sheets[55] are composed of numerous nanoflakes of graphene and graphene oxides, which form a mass of nanochannels to enable the interaction of water molecules with almost all carbon atoms.

Calculations based on density functional theory with van der Waals correction show that a single water molecule adsorbed on a graphene sheet has a binding energy of ~0.2 eV, with 0.008 electrons transferred from graphene to water (Fig. 2c). When graphene is functionalized by a hydroxyl group, the Coulomb interaction between the water molecule and graphene is enhanced, which raises the binding energy to ~0.4 eV and the corresponding charge transfer to 0.014*e* (Fig. 2c). Enhanced binding of water also occurs at the defects and edges of graphene. For example, a monovacancy and a hydrogenated zigzag edge can donate 0.024 and 0.01 electrons to each water molecule, respectively. In addition to nanochannels, carbon black sheets are rich in defects, edges and functionalized groups (Fig. 2b), thereby making them particularly suitable for interacting with water vapour, the product of evaporation.

In aqueous solutions, ions dominate the interaction with graphene. First-principles calculations show that isolated cations stick

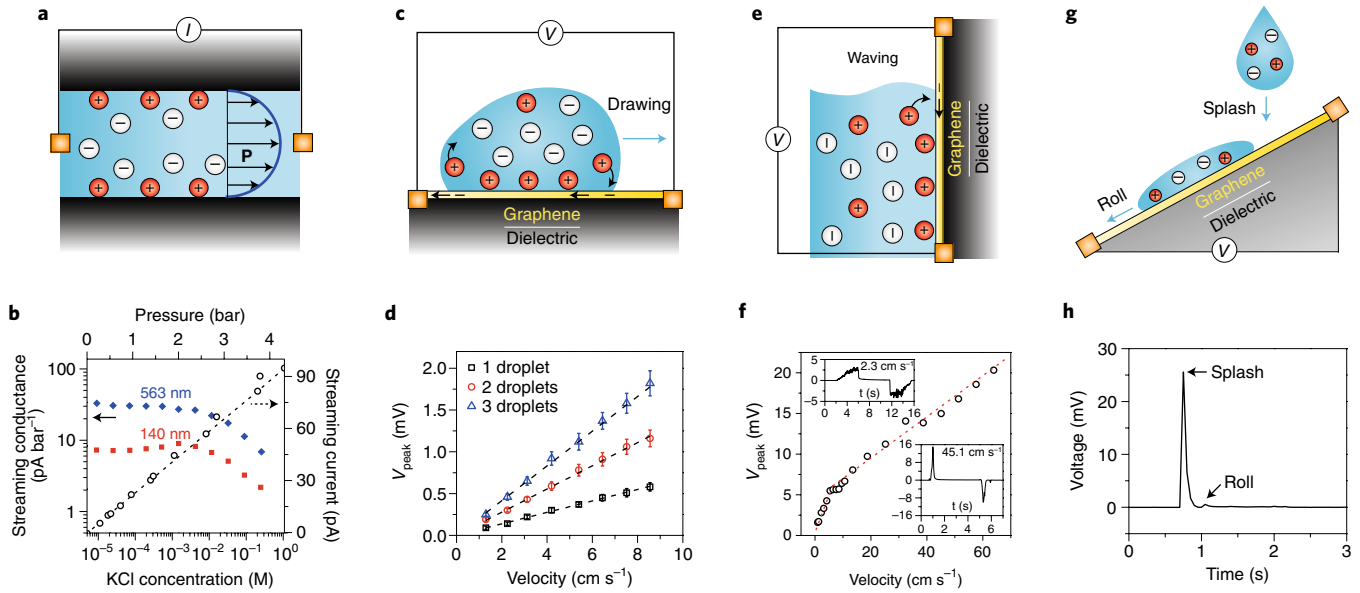

Fig. 3 | Electricity generation related to electrokinetic effects. a, Schematic illustration of classical electrokinetic effect in a nanochannel, in which the double layer overlaps and a pressure-driven flow carries counter-ions to form an electric current in the flow. Blue line shows the profile of flow velocity across the channel. **b**, Dependence of streaming conductance in different-sized channels on the solute concentration (filled symbols), and streaming current as a linear function of pressure (open symbols and dashed line). **c**, Illustration of induced potential by drawing a droplet on graphene. An electric current is formed in graphene by two moving boundaries of the double layer at the front and rear of the running droplet, respectively. **d**, Linear dependences of peak voltage on the moving velocity of one, two and three droplets. **e**, Illustration of waving potential induced in graphene by one moving boundary of the double layer across a graphene sheet on a dielectric substrate. **f**, Dependence of induced peak voltage on the velocity of the moving boundary. Insets report detailed electric signals at moving velocities of 2.3 and 45.1 cm s^{-1}, respectively. **g**, Schematic illustration of harvesting energy from raindrops. **h**, Electric signal induced by a droplet of 0.6 M $CuCl_2$ solution falling onto a tilted graphene sheet. The signals induced by splash and rolling of droplets are indicated by arrows. Figure adapted from: **b**, ref. [4], APS; and reproduced from: **f**, ref. [17] under a Creative Commons license (https://creativecommons.org/licenses/by/4.0/); **d**,**h**, ref. [18], Springer Nature Ltd.

to a freestanding graphene sheet more readily than anions do[17]. For ions in aqueous solution, the hydration blurs this preference (Fig. 2d, left). However, in real situations, graphene needs a substrate, especially when interacting with water. Since graphene is only one atom thick, it cannot fully screen the charge of the substrate. Ions in water with opposite polarity to the substrate surface will adsorb on graphene to screen the substrate charge[56], forming an EDL on the graphene (Fig. 2d, right). The free carriers in graphene are highly responsive to the formation of EDLs owing to the good electrical conductivity and high carrier mobility of graphene.

Electricity generation by electrokinetic effects

As mentioned, when a fluid comes into contact with a charged solid, an EDL will form at the interface. The EDL is composed of a Stern layer sessile on the solid surface and a diffusion layer rich in counter-ions[38–40]. An applied external force can influence the diffusion layer so as to generate a relative motion between fluid and solid, which forms the electrokinetic effect. Initially, this effect included electrophoresis, the electric-field-induced motion of particles found in 1807[57], and electro-osmosis, the field-induced motion of fluid reported in 1809[58]. Quincke[3] observed, in 1859, that the motion of electrolytes induced by a pressure gradient through a narrow channel generates a voltage in the fluid, called the streaming potential. This represents the first electricity generated through the interfacial interaction between water and solids. Subsequently, many derived forms of streaming potential have been found, such as sedimentation potential and colloid and ion vibration potentials. Combined with carbon nanomaterials, streaming potential was recently extended to drawing and waving potentials in 2014[17,18].

Streaming potential. When water is confined in a narrow space with a size close to the Debye length of the solution, the space will be occupied mostly by counter-ions because of the overlap of EDL (Fig. 3a). Driving hydrodynamic flow through the space by a pressure gradient will transport the counter-ions downstream to form an electrical current, until a steady voltage is formed in the channel flow that will oppose further migration of ionic charges. This steady current is referred to as the streaming current[59–61], which is proportional to the flow rate, pressure gradient and channel height (Fig. 3b). A recent experiment by Dekker and co-workers[4] showed that the streaming conductance increases in relation to the decrease in solute concentration and is saturated when the concentration is below about 10^{-5} to 10^{-3} M. The charge on channel walls was suggested to govern the streaming current at low salt concentrations[4], possibly by causing rapid proton transport along the channels. The electrokinetic conversion efficiency reaches its maximum at the low salt limit[5]. However, it is peculiar that the streaming current in deionized water is even higher than that in ionized water, especially in a 563-nm-high channel (Fig. 3b).

Shrinking the channel size to nanoscale proportions increases the streaming current, owing to further enhanced EDL overlap. However, it will increase the friction between the flow and the channel wall. The energy of flow in nanochannels is largely dissipated by fluidic impedance, limiting the electrokinetic conversion efficiency to 12% in theory[5] and about 3% in experiments[4,5,62]. This friction can be reduced by using a slippery wall. Indeed, CNTs and a nanocapillary material made of multilayer graphite flakes proved to enable ultrafast water flow rate[63–66], from which flow slip lengths of up to tens of micrometres were deduced[63,65]. The predicted electrokinetic conversion efficiency for systems with such large slip lengths

could exceed 30%[67,68]. Functionalizing the CNTs and graphite flakes with chemical groups could fine-tune the streaming potential but would shorten the slip length of ionic water[69]. Moreover, theorists have suggested applying magnetic fields[70] as well as using polymer solutions[71,72] and large-sized ions[73] to increase the efficiency.

Because of the limited efficiency and power density of streaming potential, further development is needed before its extensive application. Recent advances point to additional ways of increasing the power density. The first is to shorten the channel, as the water transport scales inversely with the channel length. Water flow through a three-atom-thick MoS_2 nanopore can generate a voltage of up to tens of millivolts and a current of tens of nanoamps, driven by a salinity difference across the pore[74]. The second means is to integrate numerous nanochannels to achieve massive parallelization. CNT-based hole arrays[67] and graphene hydrogel membranes[75] have been shown to provide high power densities from water flowing in their many nanochannels. Lastly, further studies are encouraged to answer important questions regarding the nanofluidic transport at an atomic level: for example, what is the origin of the channel wall charge, and how will water molecules respond to the wall charge? Answers to these and other questions should help to guide the design of high-performance electrokinetic systems[76,77].

Drawing potential. When the ionic water is a droplet laid on graphene, the EDL is formed only in the graphene region underneath the droplet. As the droplet is drawn to move on graphene[18], the formation of EDL at the front draws image charges from graphene, while the vanishing of EDL at the rear releases image charges into graphene (Fig. 3c). The respective charging and discharging of pseudocapacitance at the front and rear of the droplet result in an electric voltage in the graphene, referred to as drawing potential[18]. The voltage V and current I are proportional to the velocity v and to the number of droplets n (Fig. 3d), expressed as $V, I \propto nC_0v$, where C_0 is the pseudocapacitance per unit area. The drawing potential can be developed to harvest raindrop energy. A splash between a falling raindrop and tilted graphene generates an electric voltage one order of magnitude higher than that induced by drawing a droplet of similar size (Fig. 3g,h)[18], attributed to the high-speed spreading of the raindrop.

Waving potential. Compared with droplets, waving water is more abundant and contains much more energy, which can be harvested in a manner similar to that of the drawing potential. As graphene is inserted through the water surface, the EDL forms a dynamic boundary at the liquid–gas boundary and leads to the charging of pseudocapacitance therein. As a result, a voltage is induced in the graphene (Fig. 3e). Pulling the graphene out of the water surface produces an inverse voltage due to a discharging process at the boundary. This wave-induced voltage was recently observed by Yin et al.[17] and called waving potential. The open-circuit voltage reaches 0.1 V with a short-circuit current of 11 μA when moving a 2 cm × 10 cm sheet of graphene across a seawater surface at a velocity of 1 m s^{-1}. Based on the EDL model, the voltage and current can be deduced to be $V = R_{sq}C_0Lv$, $I = C_0Wv$, where R_{sq} is the graphene square resistance and L and W are the length and width of the graphene sheet underwater, respectively. Thus, the voltage and current are proportional to the velocity of the sheet (Fig. 3f) and can be scaled up by series and parallel connections of multiple graphene devices, respectively.

Subsequent experiments show that the waving and drawing potentials largely depend on the substrate underneath the graphene. Polytetrafluoroethylene has a higher density of charge on its surface to induce a larger C_0 at the carbon–water interface than a polyester terephthalate substrate does, so the output power from drawing a droplet on graphene on a polytetrafluoroethylene substrate is enhanced 100 times[78]. Drawing a droplet on a piezoelectric polyvinylidene fluoride substrate introduces extra charge on the substrate surface due to the pressure of the droplet. The charging and discharging at the droplet front and rear are then enhanced, respectively, by the piezoelectric effect, inducing a total voltage of 0.1 V in the graphene even with deionized water[79]. The charge in the droplet is not limited to ions but can be extended to other charged species, such as graphene oxide nanosheets[80].

Flow-induced potentials

Many studies report flow-induced potential in carbon nanostructures beyond the scope of streaming potential. In 2001, Král and Shapiro suggested that water flow along a CNT excites a phonon wind in the tubes, which would drag free carriers in the CNT to move along the flow[14]. They further estimated[14] that a densely packed CNT layer with a width of 1 mm would generate a current of 1 mA. Inside a CNT, flowing water molecules can be aligned to induce a dynamic Coulomb field, which drags free carriers in the CNT to form a current (Fig. 2e). It seems that Sun and co-workers experimentally realized such electron drag in CNTs[16]. They detected a voltage of several millivolts in one end of an individual CNT when a current was applied to the other end of the nanotube, with the effect that water molecules were absorbed to flow inside the CNT when exposed to water vapour.

The flow-induced voltages in CNT nanofilms and graphene have provoked further interest. In 2003, Ghosh and co-workers[81] found that flowing water over CNT powder filled in a 1-mm gap between two gold electrodes could induce a millivolt voltage. They attributed the voltage to a direct forcing of the free charge carriers in CNTs by the fluctuating Coulombic field of ions[81]. This explanation was subsequently debated. However, traditional streaming potential[15] cannot explain this voltage as no pressure gradient was applied. Coulomb drag[82] is also unlikely as there is no evident alignment between the water flow and CNTs in the powder. In 2011, Dhiman et al. reported electric voltages from graphene films immersed in a flow of HCl solution[83]. Their molecular dynamics simulations suggested surface ion hopping as the origin of the electricity. Nevertheless, Yin et al.[84] found that the electric voltages were from interactions between exposed electrodes and water. No measurable voltage was observed in the graphene immersed in the flow once the electrodes were sealed. This result was later confirmed by experiments from different groups[84,85]. Therefore, the exposed electrodes and residual metal catalysts in CNTs can contribute to electricity generation and lead to widely discrepant results[86–88].

Electricity induced by natural water evaporation

In contrast to all the aforementioned electrokinetic effects that require an input of mechanical work, the hydrovoltaic effect based on natural water evaporation directly converts thermal energy from the ambient environment into electric power. In further contrast to those moving forms of water energy, evaporating water is not a direct energy carrier but a medium for converting ambient heat into electricity. Furthermore, evaporation is ubiquitous and spontaneous in terms of electricity generation, with a 'side effect' of cooling down the environment. For example, the total power of natural evaporation from lakes and reservoirs in the contiguous United States was estimated to reach 325 gigawatts, more than 69% of the US electric energy production rate in 2015[89]. These features and facts underscore the importance of developing efficient technology for harvesting the energy from natural water evaporation.

Compared with bulk ionic water, water vapour from evaporation interacts more weakly with materials. A way to strengthen the interaction is to use porous carbon materials to maximize the area of carbon–vapour interaction per unit volume. As discussed above, a candidate material is carbon black sheets, which can lift the water up through the capillary pressure of the nanochannels when partly inserted in deionized water[22]. This evaporation process under

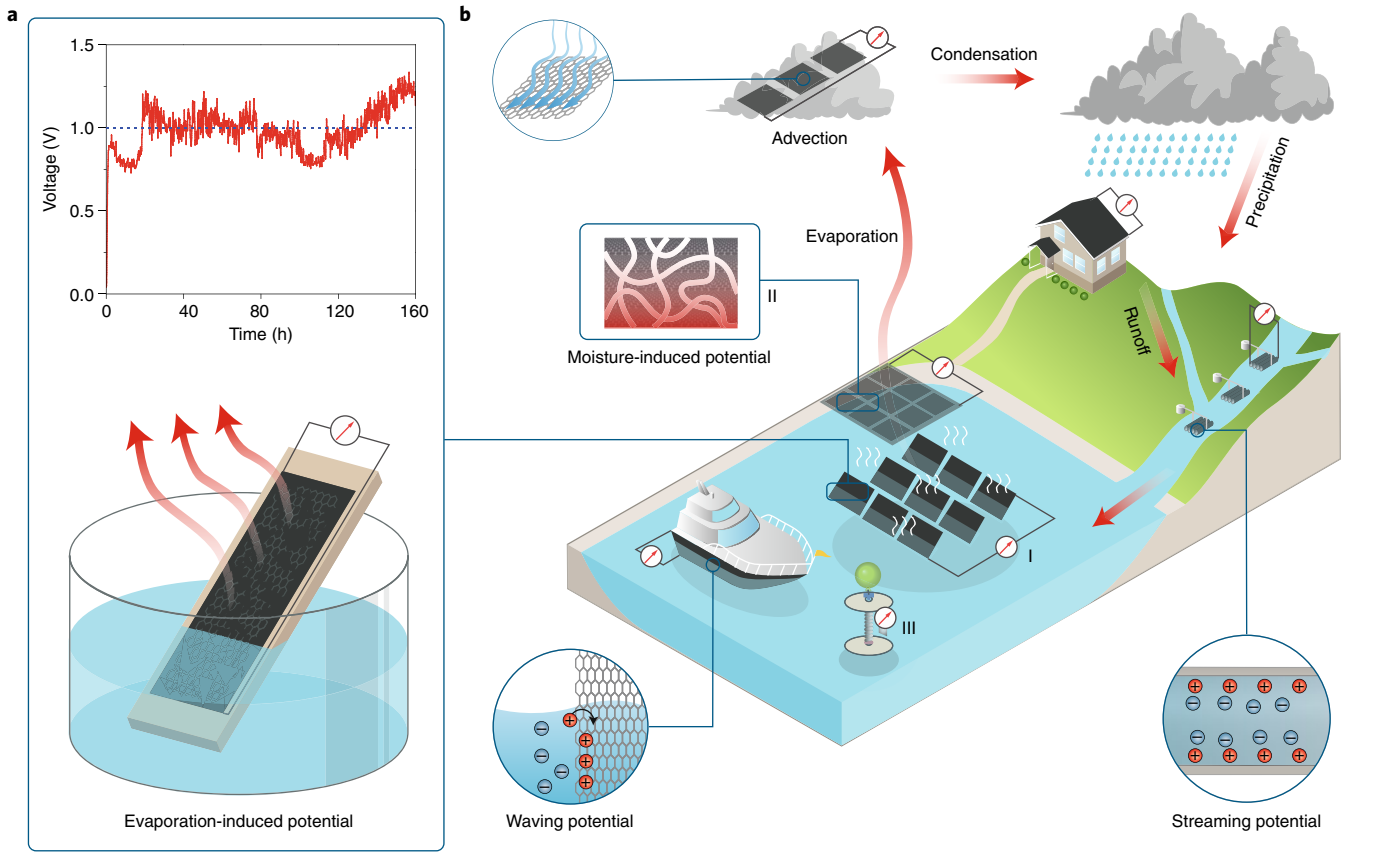

Fig. 4 | Vision of harvesting energy from the whole water cycle by carbon nanostructures. a, Carbon black sheets harvest the evaporation energy near a water surface, generating open-circuit voltage sustained for 160 h under ambient conditions. **b**, After the evaporation-induced electricity (shown in inset I and **a**), electricity can be generated from the moisture change near the water surface by using graphene oxide films (inset II; oxygen concentration decreases as the colour fades from red to grey; white lines stand for nanochannels; a power density up to 1 mW cm^{-2} can be realized in an oxide framework at a moisture variation of 80%). Then graphene sheets can harvest energy from air flow and raindrops, while graphitic capillary nanochannels can be immersed in rivers to harvest the flow energy via an illustrated mechanism of streaming potential. Finally, the energy of water waves can be harvested by adhering graphene on surfaces of floating objects based on a mechanism of waving potential as illustrated, or by attaching a carbon nanotube yarn between a balloon and a sinker on the ocean floor (inset III, an electrochemical mechanism; see text). Insets adapted from: I, ref. [22], Springer Nature Ltd; II, ref. [91], RSC; III, ref. [122], AAAS.

ambient conditions could persistently produce an electric voltage up to 1 V in a centimetre-sized carbon black sheet[22] (Fig. 4a). The induced voltage increases with the capillary length of water and then remains almost constant when the capillary water reaches a maximum height. Factors that improve the water evaporation rate, such as wind, increasing temperature and reducing relative humidity, increase the induced voltage considerably. By series and parallel connections of multiple devices, the induced electricity suffices to power commercial electric products. Ink printing can enhance the adhesion of flame-deposited carbon black sheets on substrates, making devices structurally more robust[90].

Carbon black treated by oxygen plasma contains numerous oxygen groups, for example C–O–C, C=O and O=C–OH. On contact with water, these chemical groups exchange charges with water, to an extent that is up to two orders of magnitude higher than that between water and pristine graphene, as supported by first-principles calculations[22]. The water flow driven by evaporation will create a potential gradient along the flow direction, producing an electric voltage in the carbon black sheets. Other contributions may come from the streaming potential and waving potential. The exact mechanism underlying the electricity produced in this way requires further study. There is no doubt that evaporation-induced electricity is a phenomenon beyond the traditional streaming potential. Given its many advantages over other hydrovoltaic effects, harvesting electricity from natural evaporation deserves particular attention.

Moisture-induced electricity

Evaporated water can be further controlled to form a moisture variation that presents another means of converting water to electricity, through the use of various nanostructured carbon materials such as graphene oxide materials[91–93], porous carbon films[94], and polypyrrole frameworks[95] and even TiO_2 networks with numerous charged nanochannels[96]. In particular, Qu and co-workers reported a voltage at sub-volt level and current density of tens of mA cm^{-2}, resulting in a power density up to 1 mW cm^{-2} in an oxide framework[91]. Because these carbon materials were designed to have gradients of either oxygen-containing groups (Fig. 4, inset II) or ions, the moisture-induced electricity was due to chemical gradient-driven diffusion of protons dissociated from water or of ions that unidirectionally interact with charged species in the materials under the moisture variation. Yet the exact mechanism needs to be further clarified. Graphene oxide films without chemical gradients can also produce a similar voltage but with a negligible current density of μA cm^{-2} (ref. [97]).

A couple of experiments also reported the harvesting of water vapour energy by a wet expansion effect based on materials expanding on water adsorption and contracting on desorption. Different

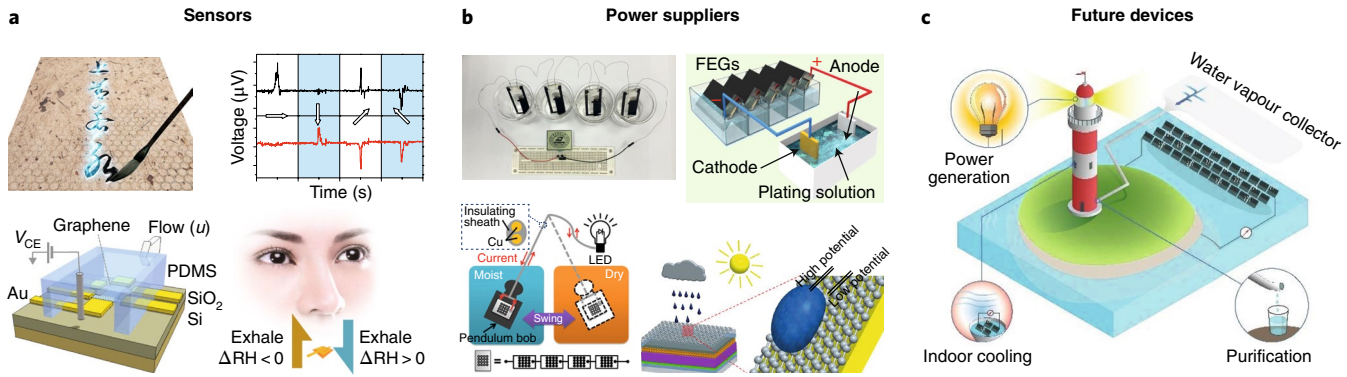

Fig. 5 | Potential device applications of water energy harvesting. a, Sensors. Top panel: a graphene sheet monitoring the writing directions of a Chinese brush. Bottom panel: a graphene field-effect transistor as a mass flow sensor (left) and a schematic illustration of a humidity sensor based on a graphene oxide film for detecting human breath (right). PDMS, polydimethylsiloxane; RH, relative humidity; V_{CE}, counter electrode voltage. **b**, Power suppliers. Top panel: evaporation-induced electricity from multiple devices connected in a series can power a liquid crystal display (left) and electro-deposition (right). FEGs, film electricity generators. Bottom left panel: moisture-activated devices made of graphene oxide films with oxygen gradients power a light-emitting diode. Each device is a series-connection of four films, as illustrated at the bottom. Bottom right panel: combining a graphene device harvesting raindrop energy with a solar cell for an all-weather energy supplier. **c**, A self-powered and self-supplied system on remote islands: evaporation-induced electricity powers the beacon light, promotes the desalination of seawater and mediates the indoor air condition. Figure reproduced from: **a**, ref. [18], Springer Nature Ltd; ref. [85], American Chemical Society; ref. [92], Wiley; **b**, ref. [22], Springer Nature Ltd; ref. [90], Wiley; ref. [91], RSC; and adapted from: **b**, ref. [124], Wiley.

from the hydrovoltaic effect, this effect outputs mechanical work in a physical manner similar to that of a steam engine, requiring a material showing a remarkable response to water vapour and a controlled large moisture variation of up to 90%. Polymer composite networks[95,98–100], liquid crystal polymers[101,102] and *Bacillus* spores[103,104] have been demonstrated to convert such moisture energy into useful mechanical energy. Pre-twisted graphene oxide fibres[105,106] also performed well in showing wetting-induced deformations that were utilized to design actuators[91,105], motors[92,106] and robots[105].

Hydrovoltaic effect in other nanomaterials

The hydrovoltaic effect is not limited to carbon nanomaterials but can be generic to other materials as long as they meet certain conditions. Taking waving and drawing potentials as examples, the material should be thin enough to allow efficient interaction between ions in water and charges on substrates (Fig. 2d). Meanwhile, it should be conductive enough for electric transport. A counter-example is multilayered graphene sheets, which are too conductive (that is, with very small R_{sq}) and severely screen the substrate charge, resulting in an electric voltage an order of magnitude lower than that in monolayer graphene[17]. Therefore, any material showing a good trade-off between thickness and conductivity is suitable for realizing waving and drawing potentials. Satisfying this criterion, doped zinc oxide nanofilms can extract electric voltages comparable to that of monolayer graphene[107] from water waves. We expect that many other semiconducting materials can be processed that will qualify as inducing the hydrovoltaic effect.

Electricity from non-hydrovoltaic effects

The hydrovoltaic effect can harvest almost all forms of water energy, but several other methods are also worth mentioning. The first is the salinity gradient energy. This type of energy is the original form of 'blue energy', available from the salinity difference between seawater and river water. The power is generated by the osmotic pressure difference between fresh and salt water and can be ultimately classified as energy of evaporation that separates fresh water from salt. The related techniques include osmosis with semipermeable membranes[108], nanofluidic diffusion with ion-selective membranes[109,110] and electric double-layer capacitors[111–113]. Further details on these techniques can be found in a recent review[114].

The second is the water energy harvesting method that uses the electrification effect combined with electrostatic induction[115–117]. This method requires dielectric materials to create charges on the surfaces of water and materials, with opposite charges then induced on two electrodes that output a voltage between them. Thus, the voltage is not from the material making direct contact with water, in contrast to the hydrovoltaic effect. There is a recent article discussing this technology[118]. Similarly, electricity can be generated by mechanically modulating water droplets confined between two parallel conducting plates, which make contact with water asymmetrically to output a voltage[119–121].

Finally, Baughman and co-workers developed an electrochemical way of harvesting wave energy using torsionally tethered coiled CNT yarns, which are immersed in an aqueous electrolyte to provide variable areas for electrochemical reactions when repeatedly stretched by water waves[122]. The electric voltage is formed between a working electrode attached to the yarns and a reference electrode in the electrolyte (Fig. 4, inset III), rather than in the carbon materials as with the waving potential. By operating the device within the ocean, voltages of tens of millivolts can be obtained, and the average electric power reaches 1.66 W kg^{-1} for wave frequencies of 0.9–1.2 Hz. Here, the water waves serve only as an external force to stretch the CNT yarns. Similar electrochemical technology can be further developed to harvest low-grade thermal energy (temperature below 130 °C)[123].

Applications and perspectives

Being able to deliver the potential in these hydrovoltaic effects and thereby transform them into practical applications is still compromised by the low output power and poor energy conversion efficiency. The output power of a single device ranges from 10^{-8} to 10^{-3} W, with a power density from 10^{-3} to 10 W m^{-2}, an output that cannot yet compete with those from conventional principles (for example, a modern water turbine can output 700 MW power with an energy efficiency over 90%). However, the electricity from the hydrovoltaic effect is already sufficient for developing self-powered devices and for powering low-consumption devices.

The drawing potential in graphene has been shown to detect water droplets or wet gas flow on its surface (Fig. 5a, top)[18,78,79], and the streaming potential has been probed by a graphene transistor

to sense mass flow and ionic concentration[85] (Fig. 5a, bottom left). A recent experiment realized a respiration monitor fabricated by graphene oxide fibres[92] and activated by moisture variation (Fig. 5a, bottom right). On the other hand, the evaporation-induced electricity from multiple devices connected in a series can power thin-film transistor displays and electro-deposition of patterned silver microstructures (Fig. 5b, top)[22,90], while moisture-induced electricity in graphene oxide films can ignite a light-emitting diode (Fig. 5b, bottom)[91]. Hybrid devices combining carbon nanomaterials with other energy conversion structures, such as dye-sensitized solar cells[124] (Fig. 5b, bottom right), silicon solar cells[125] and micro watermills, allow for an all-weather power supply. Inspired by the waving potential, Xu et al. generated electricity from the flow of blood along a CNT/polymer fibre confined in a tube, presenting a possible means for powering physiological nanodevices[126]. More broadly, harvesting the evaporation energy promises the development of self-powered and self-supplied systems on remote islands (Fig. 5c), in which the evaporation-induced electricity can be used not only to power beacon lights but also to promote evaporation[127,128] for purifying seawater. Meanwhile, the evaporation can also be implemented indoors to mediate the air condition (Fig. 5c).

Beyond these exciting applications, the ability of carbon nanostructured materials to harvest energy from air flow[129,130], waterflows[16,67,68], waves[17], raindrops[18] and evaporation[22] can help us to imagine potential ways of capturing energy from the natural water cycle. Several key processes in the cycle occurring above the ground show promise—that is, evaporation, advection, condensation, precipitation and runoff, as shown in Fig. 4. First, arrays of carbon black sheets can be installed to harvest the evaporation energy near water surfaces[22,90]. Water vapour that has permeated through the sheets can be controlled to form a moisture gradient, which can be converted into electricity by deploying a layer of water-responsive materials, such as a graphene oxide assembly[91,92] (Fig. 4, inset I). Graphene or CNTs can then harvest energy from the advection-induced air flows[129,130]. As the water vapour is condensed and precipitated, the energy of raindrops can be harvested by graphene sheets to output electric power[18]. Subsequently, the rainwater moves across the land and forms water flows along the river, which can induce the streaming potential in graphitic capillary nanochannels[16,67,68]. The water flows finally merge into ocean-forming waves, which can generate the waving potential through graphene sheets that adhere onto surfaces of any floating objects[17].

In this vision, evaporation-induced electricity stands out from other means of deriving electrical power from water, in three ways. First, water evaporation occurs everywhere and at any time, regardless of weather and environmental conditions. Second, it converts thermal energy from the ambient environment into useful electric power, without any input of mechanical work. Third, it is environmentally friendly, because its side effects (for example, reducing ambient temperature, promoting the water circle) are even a benefit. Thus, evaporation-induced electricity may hold greater potential than the photovoltaic effect. Moreover, several recent experiments have shown that evaporation can be enhanced by a synergy between plasmon-promoted solar energy absorption[131–133] and capillary-enabled rapid water diffusion[134,135]. In other words, the energy flux from the ambient environment to water vapour can be engineered to a higher level than previously supposed. These new advances make evaporation energy more relevant as a new renewable energy, even if the study of its harvesting has just begun.

But implementing the related technology on a wide scale presents several challenges. First, the carbon–water interaction is inherently weak. Each moving molecule or ion can drive only a few charge carriers in carbon nanomaterials, as shown by first-principles calculations[17]. Though functionalizing the nanomaterials enhances the carbon–water interaction, it reduces the electric conductivity and thus impedes the transport of free carriers. Second, the carbon–water interaction is limited to the surfaces of atomic layers, unlike other energy conversion processes that occur in bulk materials. Porous carbon materials can greatly increase the interaction area per unit volume, but they usually possess high internal impedance to limit electric transport. Third, parallel or series connections of multiple devices are straightforward to raise the output power. However, the power averaged from each device decreases with the increasing number of devices[17] because of interconnections among the devices and the formation of an inner loop current. Addressing this issue requires greater homogeneity of carbon materials, improved connections between devices and optimized device layout.

The above analyses indicate that a good hydrovoltaic material should achieve a balance among the following factors: strong water–carbon interaction, a large interaction area and sufficient electric conductivity. Achieving this balance is contingent on knowing the atomistic interaction mechanisms between liquid and nanostructures, which are notoriously complicated. More must be understood about the detailed dynamics involved in water and ions in liquid and carriers in materials, about the adsorption/desorption of water or ions on materials, about the dynamic coupling between ions or water and electrons at the interfaces, and about the role of substrates. Advanced computational theories and methods that enable calculations of large-scale water–solid systems at the quantum mechanical level are crucial for gaining greater insight into these issues. Moreover, experimental tools for the fine characterization of water–solid interfaces remain to be developed. Regular high-resolution microscopies work poorly for these interfaces. Instead, a relatively ordered arrangement of water and ions at the interface compared with those in bulk water allows for characterization by optical means, such as phase-sensitive sum-frequency vibrational spectroscopy[136–139].

Conclusions

Our review of electricity generation in carbon nanostructured materials interacting with water has demonstrated the great potential of harvesting water energy by using nanotechnology. Striking progress has been seen on a new effect of electrifying nanomaterials by direct coupling with water, what we have called the hydrovoltaic effect, capable of harvesting energy from water flows, waves, raindrops, evaporation and moisture. This effect is distinguished by its ability to convert the thermal energy in ambient environment to electric power through ubiquitous water evaporation. As the evaporation is uninterrupted and available under any conditions, the hydrovoltaic effect would have unique advantages over other energy conversion effects if the electric power could be enhanced to a daily usable level. This, however, is challenged by the fact that the characteristic scale of interaction strength between water and nanomaterials is at an electronvolt level, and the interaction is limited to surfaces of single atomic layers. Future study should be steered to develop theories beyond the electric double layer model for describing water–solid interfaces and explore ways of enhancing the water–material interaction, maximizing the interaction area per unit volume without sacrificing electric conductivity and combining with other energy conversion effects in a concerted manner.

Overall, compared with the century-long development of industrial hydropower, the rapid growth of hydrovoltaic voltages from original millivolt- to volt-level over the course of just a few years suggests great promise. We expect this momentum to continue with the persistent collaboration between theorists and experimenters. Furthermore, we believe that such collaboration will transform the recent focus on this emerging hydrovoltaic effect into a viable and prominent industry technology.

Received: 12 December 2017; Accepted: 12 July 2018;
Published online: 6 December 2018

References

1. Stephens, G. L. et al. An update on Earth's energy balance in light of the latest global observations. *Nat. Geosci.* **5**, 691–696 (2012).
2. Dudley, B. *Statistical Review of World Energy* (BP, 2017).
3. Wall, S. The history of electrokinetic phenomena. *Curr. Opin. Colloid Interface Sci.* **15**, 119–124 (2010).
4. Van der Heyden, F. H., Stein, D. & Dekker, C. Streaming currents in a single nanofluidic channel. *Phys. Rev. Lett.* **95**, 116104 (2005).
This paper reported the dependence of streaming currents on salt concentration of water flow in nanochannels and observed peculiar behaviour at the low-salt limit.
5. Van der Heyden, F. H., Bonthuis, D. J., Stein, D., Meyer, C. & Dekker, C. Electrokinetic energy conversion efficiency in nanofluidic channels. *Nano Lett.* **6**, 2232–2237 (2006).
6. Daiguji, H., Yang, P., Szeri, A. J. & Majumdar, A. Electrochemomechanical energy conversion in nanofluidic channels. *Nano Lett.* **4**, 2315–2321 (2004).
7. Sparreboom, W. V., Van Den Berg, A. & Eijkel, J. Principles and applications of nanofluidic transport. *Nat. Nanotech.* **4**, 713–720 (2009).
8. Zhang, S. et al. Arrays of horizontal carbon nanotubes of controlled chirality grown using designed catalysts. *Nature* **543**, 234–238 (2017).
9. Yang, F. et al. Chirality-specific growth of single-walled carbon nanotubes on solid alloy catalysts. *Nature* **510**, 522–524 (2014).
10. Xu, X. et al. Ultrafast epitaxial growth of metre-sized single-crystal graphene on industrial Cu foil. *Sci. Bull.* **62**, 1074–1080 (2017).
11. Chen, Z. et al. Three-dimensional flexible and conductive interconnected graphene networks grown by chemical vapour deposition. *Nat. Mater.* **10**, 424–428 (2011).
12. Sun, H., Xu, Z. & Gao, C. Multifunctional, ultra-flyweight, synergistically assembled carbon aerogels. *Adv. Mater.* **25**, 2554–2560 (2013).
13. Cao, A., Dickrell, P. L., Sawyer, W. G., Ghasemi-Nejhad, M. N. & Ajayan, P. M. Super-compressible foamlike carbon nanotube films. *Science* **310**, 1307–1310 (2005).
14. Král, P. & Shapiro, M. Nanotube electron drag in flowing liquids. *Phys. Rev. Lett.* **86**, 131 (2001).
15. Cohen, A. E. Carbon nanotubes provide a charge. *Science* **300**, 1235–1236 (2003).
16. Zhao, Y. et al. Individual water-filled single-walled carbon nanotubes as hydroelectric power converters. *Adv. Mater.* **20**, 1772–1776 (2008).
This paper demonstrated the first experimental evidence of electric voltage induced by flowing water inside a single-walled carbon nanotube.
17. Yin, J. et al. Waving potential in graphene. *Nat. Commun.* **5**, 3582 (2014).
This paper was the first to demonstrate electricity generation in a graphene sheet by moving a liquid–gas boundary along the sheet.
18. Yin, J. et al. Generating electricity by moving a droplet of ionic liquid along graphene. *Nat. Nanotech.* **9**, 378–383 (2014).
This paper was the first experimental work to show that moving a droplet of ionic water along graphene generates electric voltage in the graphene.
19. Liu, Z. Advances in electrokinetics revealed in graphene. *Natl Sci. Rev.* **2**, 17–18 (2015).
20. Penman, H. L. Natural evaporation from open water, bare soil and grass. *Proc. R. Soc. Lond. A* **193**, 120–145 (1948).
21. Trenberth, K. E., Fasullo, J. T. & Kiehl, J. Earth's global energy budget. *Bull. Am. Meteorol. Soc.* **90**, 311–323 (2009).
22. Xue, G. et al. Water-evaporation-induced electricity with nanostructured carbon materials. *Nat. Nanotech.* **12**, 317–321 (2017).
This paper was the first to realize energy harvesting from natural water evaporation using carbon nanostructured materials.
23. Luque, A. & Hegedus, S. (eds) *Handbook of Photovoltaic Science and Engineering* (Wiley, Chichester, 2011).
24. Gregory, J., Clary, D., Liu, K., Brown, M. & Saykally, R. The water dipole moment in water clusters. *Science* **275**, 814–817 (1997).
25. Eisenberg, D. & Kauzmann, W. *The Structure and Properties of Water* (Oxford Univ. Press, Oxford, 1969).
26. Feyereisen, M. W., Feller, D. & Dixon, D. A. Hydrogen bond energy of the water dimer. *J. Chem. Phys.* **100**, 2993–2997 (1996).
27. Israelachvili, J. N. *Intermolecular and Surface Forces* (Academic Press, Cambridge, MA, 2011).
28. Eigen, M. & Maeyer, L. D. Self-dissociation and protonic charge transport in water and ice. *Proc. R. Soc. Lond. A* **247**, 505–533 (1958).
29. Marx, D., Tuckerman, M. E., Hutter, J. & Parrinello, M. The nature of the hydrated excess proton in water. *Nature* **397**, 601–604 (1999).
30. Habershon, S., Markland, T. E. & Manolopoulos, D. E. Competing quantum effects in the dynamics of a flexible water model. *J. Chem. Phys.* **131**, 024501 (2009).
31. Tuckerman, M. E., Marx, D., Klein, M. L. & Parrinello, M. On the quantum nature of the shared proton in hydrogen bonds. *Science* **275**, 817–820 (1997).
32. Fang, W., Richardson, J. O., Chen, J., Li, X.-Z. & Michaelides, A. Simultaneous deep tunneling and classical hopping for hydrogen diffusion on metals. *Phys. Rev. Lett.* **119**, 126001 (2017).
33. Chen, J. et al. Quantum simulation of low-temperature metallic liquid hydrogen. *Nat. Commun.* **4**, 2064 (2013).
34. Blum, W. et al. Clinical response and miR-29b predictive significance in older AML patients treated with a 10-day schedule of decitabine. *Proc. Natl Acad. Sci. USA* **107**, 7473–7478 (2010).
35. Ceriotti, M. et al. Nuclear quantum effects in water and aqueous systems: experiment, theory, and current challenges. *Chem. Rev.* **116**, 7529–7550 (2016).
36. Zheng, J.-M., Chin, W.-C., Khijniak, E., Khijniak, E. & Pollack, G. H. Surfaces and interfacial water: evidence that hydrophilic surfaces have long-range impact. *Adv. Colloid Interface Sci.* **127**, 19–27 (2006).
37. Henderson, M. A. The interaction of water with solid surfaces: fundamental aspects revisited. *Surf. Sci. Rep.* **46**, 5–308 (2002).
38. Block, L. P. A double layer review. *Astrophys. Space Sci.* **55**, 59–83 (1978).
39. Carnie, S. L. & Torrie, G. M. The statistical mechanics of the electrical double layer. *Adv. Chem. Phys.* **56**, 141–253 (2007).
40. Grahame, D. C. The electrical double layer and the theory of electrocapillarity. *Chem. Rev.* **41**, 441–501 (1947).
41. Hunter, R. J. *Zeta Potential in Colloid Science: Principles and Applications* (Academic Press, Cambridge, MA, 2013).
42. Gustafsson, J., Mikkola, P., Jokinen, M. & Rosenholm, J. B. The influence of pH and NaCl on the zeta potential and rheology of anatase dispersions. *Colloids Surf. A* **175**, 349–359 (2000).
43. Maier, J. Thermodynamic aspects and morphology of nano-structured ion conductors: aspects of nano-ionics Part I. *Solid State Ionics* **154**, 291–301 (2002).
44. Zhang, Z. et al. Tunable electronic and magnetic properties of two-dimensional materials and their one-dimensional derivatives. *Wiley Interdiscip. Rev. Comput. Mol. Sci.* **6**, 324–350 (2016).
45. Wallace, P. R. The band theory of graphite. *Phys. Rev.* **71**, 622 (1947).
46. Novoselov, K. S. et al. Two-dimensional gas of massless Dirac fermions in graphene. *Nature* **438**, 197–200 (2005).
47. Koga, K., Tanaka, H. & Zeng, X. First-order transition in confined water between high-density liquid and low-density amorphous phases. *Nature* **408**, 564–567 (2000).
48. Koga, K., Gao, G., Tanaka, H. & Zeng, X. C. Formation of ordered ice nanotubes inside carbon nanotubes. *Nature* **412**, 802–805 (2001).
49. Liu, Y. & Wang, Q. Transport behavior of water confined in carbon nanotubes. *Phys. Rev. B* **72**, 085420 (2005).
50. Alexiadis, A. & Kassinos, S. Molecular simulation of water in carbon nanotubes. *Chem. Rev.* **108**, 5014–5034 (2008).
51. Yuan, Q. & Zhao, Y.-P. Hydroelectric voltage generation based on water-filled single-walled carbon nanotubes. *J. Am. Chem. Soc.* **131**, 6374–6376 (2009).
52. Dellago, C., Naor, M. M. & Hummer, G. Proton transport through water-filled carbon nanotubes. *Phys. Rev. Lett.* **90**, 105902 (2003).
53. Jiang, K., Li, Q. & Fan, S. Spinning continuous carbon nanotube yarns. *Nature* **419**, 801–801 (2002).
54. Zhang, M., Atkinson, K. R. & Baughman, R. H. Multifunctional carbon nanotube yarns by downsizing an ancient technology. *Science* **306**, 1358–1361 (2004).
55. Donnet, J.-B. *Carbon Black: Science and Technology* (CRC, Boca Raton, 1993).
56. Yang, S. et al. Mechanism of electric power generation from ionic droplet motion on polymer supported graphene. Preprint at https://arxiv.org/abs/1801.07878 (2018).
57. Reuss, F. F. Sur un nouvel effet de l'électricité galvanique. *Mem. Soc. Imp. Natur. Moscou* **2**, 327–337 (1809).
58. Reuss, F. Charge-induced flow. *Proc. Imperial Soc. Naturalists Mosc.* **3**, 327–344 (1809).
59. Stone, H. A., Stroock, A. D. & Ajdari, A. Engineering flows in small devices: microfluidics toward a lab-on-a-chip. *Annu. Rev. Fluid Mech.* **36**, 381–411 (2004).
60. Graetz, M. V. S. I. Handbuch der Elektrizitat und des Magnetismus. *Leipzig* **11**, 366 (1914).
61. Hunter, R. J. *Foundations of Colloid Science* (Oxford Univ. Press, Oxford, 1995).
62. Van der Heyden, F. H., Bonthuis, D. J., Stein, D., Meyer, C. & Dekker, C. Power generation by pressure-driven transport of ions in nanofluidic channels. *Nano Lett.* **7**, 1022–1025 (2007).
63. Holt, J. K. et al. Fast mass transport through sub-2-nanometer carbon nanotubes. *Science* **312**, 1034–1037 (2006).
64. Radha, B. et al. Molecular transport through capillaries made with atomic-scale precision. *Nature* **538**, 222 (2016).
65. Majumder, M., Chopra, N., Andrews, R. & Hinds, B. J. Nanoscale hydrodynamics: enhanced flow in carbon nanotubes. *Nature* **438**, 44 (2005).

66. Thomas, J. A. & McGaughey, A. J. Water flow in carbon nanotubes: transition to subcontinuum transport. *Phys. Rev. Lett.* **102**, 184502 (2009).
67. Ren, Y. & Stein, D. Slip-enhanced electrokinetic energy conversion in nanofluidic channels. *Nanotechnology* **19**, 195707 (2008).
68. Author, A. Energy conversion in microsystems: is there a role for micro/nanofluidics? *Lab Chip* **7**, 1234–1237 (2007).
69. Wei, N., Peng, X. & Xu, Z. Breakdown of fast water transport in graphene oxides. *Phys. Rev. E* **89**, 012113 (2014).
70. Munshi, F. & Chakraborty, S. Hydroelectrical energy conversion in narrow confinements in the presence of transverse magnetic fields with electrokinetic effects. *Phys. Fluids* **21**, 122003 (2009).
71. Nguyen, T., Xie, Y., de Vreede, L. J., van den Berg, A. & Eijkel, J. C. T. Highly enhanced energy conversion from the streaming current by polymer addition. *Lab Chip* **13**, 3210–3216 (2013).
72. Berli, C. L. A. Electrokinetic energy conversion in microchannels using polymer solutions. *J. Colloid Interface Sci.* **349**, 446–448 (2010).
73. Gillespie, D. High energy conversion efficiency in nanofluidic channels. *Nano Lett.* **12**, 1410–1416 (2012).
74. Feng, J. et al. Single-layer MoS_2 nanopores as nanopower generators. *Nature* **536**, 197–200 (2016).
75. Guo, W. et al. Bio-inspired two-dimensional nanofluidic generators based on a layered graphene hydrogel membrane. *Adv. Mater.* **25**, 6064–6068 (2013).
76. Esfandiar, A. et al. Size effect in ion transport through angstrom-scale slits. *Science* **358**, 511–513 (2017).
77. Siria, A. et al. Giant osmotic energy conversion measured in a single transmembrane boron nitride nanotube. *Nature* **494**, 455–458 (2013).
78. Kwak, S. S. et al. Triboelectrification-induced large electric power generation from a single moving droplet on graphene/polytetrafluoroethylene. *ACS Nano* **10**, 7297–7302 (2016).
79. Zhong, H. et al. Graphene-piezoelectric material heterostructure for harvesting energy from water flow. *Adv. Funct. Mater.* **27**, 1104226 (2017).
80. Zhong, H. et al. Two dimensional graphene nanogenerator by Coulomb dragging: moving van der Waals heterostructure. *Appl. Phys. Lett.* **106**, 243903 (2015).
81. Cohen, A. E., Ghosh, S., Sood, A. & Kumar, N. Carbon nanotube flow sensors. *Science* **299**, 1042–1044 (2003).
This paper showed that flowing water over CNT powder filled in a gap between two electrodes could induce a millivolt voltage.
82. Ghosh, S., Sood, A. K., Ramaswamy, S. & Kumar, N. Flow-induced voltage and current generation in carbon nanotubes. *Phys. Rev. B* **70**, 205423 (2004).
83. Dhiman, P. et al. Harvesting energy from water flow over graphene. *Nano Lett.* **11**, 3123–3127 (2011).
84. Yin, J., Zhang, Z., Li, X., Zhou, J. & Guo, W. Harvesting energy from water flow over graphene? *Nano Lett.* **12**, 1736–1741 (2012).
This paper revealed for the first time important role of bare electrodes in generating electricity in carbon nanomaterials immersed in flowing water.
85. Newaz, A. K. M., Markov, D. A., Prasai, D. & Bolotin, K. I. Graphene transistor as a probe for streaming potential. *Nano Lett.* **12**, 2931–2935 (2012).
86. Liu, J., Dai, L. & Baur, J. W. Multiwalled carbon nanotubes for flow-induced voltage generation. *J. Appl. Phys.* **101**, 064312 (2007).
87. Lee, S. H., Kim, D., Kim, S. & Han, C.-S. Flow-induced voltage generation in high-purity metallic and semiconducting carbon nanotubes. *Appl. Phys. Lett.* **99**, 104103 (2011).
88. Persson, B., Tartaglino, U., Tosatti, E. & Ueba, H. Electronic friction and liquid-flow-induced voltage in nanotubes. *Phys. Rev. B* **69**, 235410 (2004).
89. Cavusoglu, A.-H., Chen, X., Gentine, P. & Sahin, O. Potential for natural evaporation as a reliable renewable energy resource. *Nat. Commun.* **8**, 617 (2017).
90. Ding, T. et al. All-printed porous carbon film for electricity generation from evaporation-driven water flow. *Adv. Funct. Mater.* **27**, 1700551 (2017).
91. Zhao, F., Liang, Y., Cheng, H., Jiang, L. & Qu, L. Highly efficient moisture-enabled electricity generation from graphene oxide frameworks. *Energy Environ. Sci.* **9**, 912–916 (2016).
92. Zhao, F., Cheng, H., Zhang, Z., Jiang, L. & Qu, L. Direct power generation from a graphene oxide film under moisture. *Adv. Mater.* **27**, 4351–4357 (2015).
93. Liang, Y. et al. Electric power generation via asymmetric moisturizing of graphene oxide for flexible, printable and portable electronics. *Energy Environ. Sci.* **11**, 1730–1735 (2018).
94. Liu, K. et al. Induced potential in porous carbon films through water vapor absorption. *Angew. Chem. Int. Ed.* **128**, 8135–8139 (2016).
95. Xue, J. et al. Vapor-activated power generation on conductive polymer. *Adv. Funct. Mater.* **26**, 8784–8792 (2016).
Refs 91–95 realized power generation based on moisture variation across carbon nanomaterials with a gradient of chemical groups.
96. Shen, D. et al. Self-powered wearable electronics based on moisture enabled electricity generation. *Adv. Mater.* **30**, 1705925 (2018).
97. Xu, T. et al. Electric power generation through the direct interaction of pristine graphene-oxide with water molecules. *Small* **14**, 1704473 (2018).
98. Ma, M., Guo, L., Anderson, D. G. & Langer, R. Bio-inspired polymer composite actuator and generator driven by water gradients. *Science* **339**, 186–189 (2013).
99. Kim, H. & Kwon, S. Water-responsive polymer composites on the move. *Science* **339**, 150–151 (2013).
100. Arazoe, H. et al. An autonomous actuator driven by fluctuations in ambient humidity. *Nat. Mater.* **15**, 1084–1089 (2016).
101. De Haan, L. T., Verjans, J. M., Broer, D. J., Bastiaansen, C. W. & Schenning, A. P. Humidity-responsive liquid crystalline polymer actuators with an asymmetry in the molecular trigger that bend, fold, and curl. *J. Am. Chem. Soc.* **136**, 10585–10588 (2014).
102. Zhao, Q. et al. Sensing solvents with ultrasensitive porous poly (ionic liquid) actuators. *Adv. Mater.* **27**, 2913–2917 (2015).
103. Chen, X., Mahadevan, L., Driks, A. & Sahin, O. Bacillus spores as building blocks for stimuli-responsive materials and nanogenerators. *Nat. Nanotech.* **9**, 137–141 (2014).
104. Chen, X. et al. Scaling up nanoscale water-driven energy conversion into evaporation-driven engines and generators. *Nat. Commun.* **6** (2015).
105. Cheng, H. et al. Graphene fibers with predetermined deformation as moisture-triggered actuators and robots. *Angew. Chem. Int. Ed.* **52**, 10482–10486 (2013).
106. Cheng, H. et al. Moisture-activated torsional graphene-fiber motor. *Adv. Mater.* **26**, 2909–2913 (2014).
107. Li, X. et al. Hydroelectric generator from transparent flexible zinc oxide nanofilms. *Nano Energy* **32**, 125–129 (2017).
108. Levenspiel, O. & de Nevers, N. The osmotic pump. *Science* **183**, 157–160 (1974).
109. Weinstein, J. N. & Leitz, F. B. Electric power from differences in salinity: the dialytic battery. *Science* **191**, 557–559 (1976).
110. Gao, J. et al. High-performance ionic diode membrane for salinity gradient power generation. *J. Am. Chem. Soc.* **136**, 12265–12272 (2014).
111. Brogioli, D. Extracting renewable energy from a salinity difference using a capacitor. *Phys. Rev. Lett.* **103**, 058501 (2009).
112. Brogioli, D., Zhao, R. & Biesheuvel, P. A prototype cell for extracting energy from a water salinity difference by means of double layer expansion in nanoporous carbon electrodes. *Energy Environ. Sci.* **4**, 772–777 (2011).
113. La Mantia, F., Pasta, M., Deshazer, H. D., Logan, B. E. & Cui, Y. Batteries for efficient energy extraction from a water salinity difference. *Nano Lett.* **11**, 1810–1813 (2011).
114. Jia, Z., Wang, B., Song, S. & Fan, Y. Blue energy: current technologies for sustainable power generation from water salinity gradient. *Renew. Sust. Energy Rev.* **31**, 91–100 (2014).
115. Lin, Z. H., Cheng, G., Lin, L., Lee, S. & Wang, Z. L. Water–solid surface contact electrification and its use for harvesting liquid-wave energy. *Angew. Chem. Int. Ed.* **52**, 12545–12549 (2013).
116. Park, J., Yang, Y., Kwon, S.-H. & Kim, Y. S. Influences of surface and ionic properties on electricity generation of an active transducer driven by water motion. *J. Phys. Chem. Lett.* **6**, 745–749 (2015).
117. Han, M. et al. Electrification based devices with encapsulated liquid for energy harvesting, multifunctional sensing, and self-powered visualized detection. *J. Mater. Chem. A* **3**, 7382–7388 (2015).
118. Wang, Z. L. Catch wave power in floating nets. *Nature* **542**, 159–160 (2017).
119. Moon, J. K., Jeong, J., Lee, D. & Pak, H. K. Electrical power generation by mechanically modulating electrical double layers. *Nat. Commun.* **4**, 2485 (2013).
120. Liu, K. et al. Self-powered multimodal temperature and force sensor based on a liquid droplet. *Angew. Chem. Int. Ed.* **128**, 16096–16100 (2016).
121. Kwon, S.-H. et al. An effective energy harvesting method from a natural water motion active transducer. *Energy Environ. Sci.* **7**, 3279–3283 (2014).
122. Kim, S. H. et al. Harvesting electrical energy from carbon nanotube yarn twist. *Science* **357**, 773–778 (2017).
123. Hu, R. et al. Harvesting waste thermal energy using a carbon-nanotube-based thermo-electrochemical cell. *Nano Lett.* **10**, 838–846 (2010).
124. Tang, Q., Wang, X., Yang, P. & He, B. A solar cell that is triggered by sun and rain. *Angew. Chem. Int. Ed.* **55**, 5243–5246 (2016).
125. Zhong, H. et al. Graphene based two dimensional hybrid nanogenerator for concurrently harvesting energy from sunlight and water flow. *Carbon* **105**, 199–204 (2016).
Refs 124 and 125 demonstrated integration of hydrovoltaic devices with solar cells for realizing all-weather power supply.
126. Xu, Y. et al. A one-dimensional fluidic nanogenerator with a high power conversion efficiency. *Angew. Chem. Int. Ed.* **56**, 12940–12945 (2017).
127. Zhang, P., Li, J., Lv, L., Zhao, Y. & Qu, L. Vertically aligned graphene sheets membrane for highly efficient solar thermal generation of clean water. *ACS Nano* **11**, 5087–5093 (2017).

128. Lou, J. et al. Bioinspired multifunctional paper-based rGO composites for solar-driven clean water generation. *ACS Appl. Mater. Interfaces* **8**, 14628–14636 (2016).
129. Yin, J. et al. Enhanced gas-flow-induced voltage in graphene. *Appl. Phys. Lett.* **99**, 073103 (2011).
130. Sood, A. & Ghosh, S. Direct generation of a voltage and current by gas flow over carbon nanotubes and semiconductors. *Phys. Rev. Lett.* **93**, 086601 (2004).
131. Zhou, L. et al. 3D self-assembly of aluminium nanoparticles for plasmon-enhanced solar desalination. *Nat. Photon* **10**, 393–398 (2016).
132. Bae, K. et al. Flexible thin-film black gold membranes with ultrabroadband plasmonic nanofocusing for efficient solar vapour generation. *Nat. Commun.* **6**, 10103 (2015).
133. Liu, Y. et al. A bioinspired, reusable, paper-based system for high-performance large-scale evaporation. *Adv. Mater.* **27**, 2768–2774 (2015).
134. Zhao, F. et al. Highly efficient solar vapour generation via hierarchically nanostructured gels. *Nat. Nanotech.* **13**, 489–495 (2018).
135. Ito, Y. et al. Multifunctional porous graphene for high-efficiency steam generation by heat localization. *Adv. Mater.* **27**, 4302–4307 (2015).
136. Ostroverkhov, V., Waychunas, G. A. & Shen, Y. New information on water interfacial structure revealed by phase-sensitive surface spectroscopy. *Phys. Rev. Lett.* **94**, 046102 (2005).
137. Ji, N., Ostroverkhov, V., Chen, C.-Y. & Shen, Y.-R. Phase-sensitive sum-frequency vibrational spectroscopy and its application to studies of interfacial alkyl chains. *J. Am. Chem. Soc.* **129**, 10056–10057 (2007).
138. Ji, N., Ostroverkhov, V., Tian, C. & Shen, Y. Characterization of vibrational resonances of water-vapor interfaces by phase-sensitive sum-frequency spectroscopy. *Phys. Rev. Lett.* **100**, 096102 (2008).
139. Tian, C. S. & Shen, Y. R. Structure and charging of hydrophobic material/water interfaces studied by phase-sensitive sum-frequency vibrational spectroscopy. *Proc. Natl Acad. Sci. USA* **106**, 15148–15153 (2009).

Acknowledgements

This work was supported by the National Natural Science Foundation of China (grant nos. 51535005, 11772153, 51472117, 51702159), the Research Fund of State Key Laboratory of Mechanics and Control of Mechanical Structures (MCMS-0416K01, MCMS-0416G01, MCMS-0417G01), the Fundamental Research Funds for the Central Universities (NP2017101, NE2018002), a Project Funded by the Priority Academic Program Development of Jiangsu Higher Education Institutions, and the support of the Sugon Scholarship. Z.Z. also acknowledges the support of Youth Thousand Talents Program.

Competing interests

The authors declare no competing interests.

Additional information

Reprints and permissions information is available at www.nature.com/reprints.

Correspondence should be addressed to W.G.

Publisher's note: Springer Nature remains neutral with regard to jurisdictional claims in published maps and institutional affiliations.